UNBALANCE IDENTIFICATION IN ROTATING MACHINERY APPLYING A MULTI-OBJECTIVE METAHEURISTIC METHOD

Lucas Ward Franco de Camargo, lucaswfc@gmail.com
Helio Fiori de Castro, heliofc@fem.unicamp.br
Katia Lucchesi Cavalca, katia@fem.unicamp.br
Laboratory of Rotating Machinery – Faculty of Mechanical Engineering – Postal Box 6122
University of Campinas – UNICAMP – 13083-970, Campinas, SP, Brazil

Abstract. *This paper presents a non-linear model updating applying multi-objective genetic algorithm as searching method, in order to obtain the tuning of mathematical model parameters in rotating systems. An experimental set up for this purpose consists of a rotor on a rigid foundation supported by two cylindrical journal bearings and with a central disk of considerable mass and a coupling between drive-motor and shaft. A finite element model is used to simulate rotor and shaft. The ideal symmetric rotor model is carried out for this problem and the excitation force is due to an unbalanced mass and its eccentricity and phase. The journal bearings are modeled through a non-linear force expression. As some parameters of the analytical dynamic model of the system are unknown, or even approached, the model needs to be adjusted to accurately simulate the real structure. This problem involves the simultaneous solution of multiple performance criteria. A multi-objective genetic algorithm is, then, proposed to allow the individual analysis of each objective function, which are based on the difference between the geometric properties of the experimental and simulated elliptical orbits. The parameters considered as unknown, which are adjusted by the optimization process, are the unbalance (position, phase and magnitude) and the load on each bearing. Several shaft rotations are considered in the fitting process, so that the results can be applied to a large operational range of the machine. The use of the multi-objective optimization approach returns a Pareto optimal set of solutions (Pareto front) where the identification of the best one is not possible. Using high level information, it is possible to choose between these solutions and fit the mathematical model to obtain reliable responses for the studied physical system. In this paper, the multi-objective algorithm is based on the multi-objective genetic algorithm SPEA (Strength Pareto Evolutionary Algorithm). This research also proposes a contribution for the rotating machine design area as it presents a relatively simple method of tuning and validation of computational models for machines and structures, considering the conflicting aspects of the parameters used on the objective functions.*

Keywords*: Journal bearing, Model Tuning, Rotordynamics, Multi-Objective Genetic Algorithm*

1. INTRODUCTION

The study of rotating machines occupies a special position in the context of machines and structures, in view of the considerable amount of typical phenomena in the operation of those equipments. The existence of a rotary component supported on bearings and transmitting power creates numerous problems that affect a wide variety of machines, i.e., compressors, pumps, motors, large and small turbines, etc. Mathematical models are developed to foresee the dynamic behavior of those systems. However, analytical and experimental results still show discrepancies due to a lack of knowledge of several parameters inherent to dynamic systems and due to simplifications in these models. This way, to obtain reliable results, it is necessary to use updating techniques to adjust the results of the simulations of the models to those obtained in experimental tests.

The first studies on the influence of the dynamic behavior of bearings in rotating machinery (hydrodynamic lubrication theory) were done by Tower (1883 and 1885). Reynolds (1886) established the differential equation for the pressure profile of two surfaces in relative movement due to the internal pressure variation of the fluid film between the surfaces. Lund (1987) presented the concept of dynamic (stiffness and damping) coefficients and this linear model approach is highly applied for rotor-bearing systems. However, this approach is not able to provide information about the nonlinearities inherent to these components and its application can be unsatisfactory for many applications and frequency ranges. Capone (1986 and 1991) studied a nonlinear model of the hydrodynamic supporting efforts in lubricated bearings, valid for short bearings in a laminar flux condition. This way, the time-domain response of a rotary system (taking into account the nonlinearities of the system) can be obtained. In order to validate Capone´s model, Cavalca *et al.* (2001) compared simulated efforts in the bearing to experimental data and obtained the oil film temperature in the bearings.

Capone´s formulation for short cylindrical journal bearings is applied in this work, as part of a rotary system modeled by a finite element method. The unknown parameters considered in the system are the unbalance components (magnitude, phase and position), as well as the load on each bearing. In order to identify these parameters, simulated and experimental data are compared and a multi-objective metaheuristic search method, based on genetic algorithm, is proposed. Experimental data was obtained in a laboratory bench-scale rotor-bearing system and acquired for four constant rotations close to the system´s critical range of operation (critical speed).

The genetic algorithm (Holland, 1975 and Goldberg, 1989) is a search technique based on concepts of biological evolution and reproduction, which can be applied to solve several engineering problems. Previous works indicate that genetic algorithms are recommended for problems involving complex mathematical expressions in their modeling.

Castro *et al.* (2004 and 2005) studied a rotor-bearing system in which the unknown parameters were the unbalance magnitude and the viscosity in the bearings. A single objective fitting process, based on genetic algorithm, was considered. Weights were chosen for each one of the objective function, representing the importance of each parameter in the adjustment process, in order to describe the problem using only one objective function. This way, only a single solution was obtained for each set of weights. A better refinement of the results was obtained by Castro and Cavalca (2007) with a hybrid procedure combining two metaheuristic approaches: the genetic algorithm and the Simulated Annealing (Kirkpatrick, 1982), in which the solutions found by the genetic algorithm were used as input for the Simulated Annealing.

To improve the search method, Castro *et al.* (2008) applied the Multi-Objective Genetic Algorithm *MOGA* (Fonseca and Fleming, 1993) to a similar problem in order to evaluate independently the three objective functions and obtain a Pareto optimal set of solutions. As the algorithm considers each objective function separately, there is no need for the weight selection. Zitzler *et al.* (2000) presented a comparative study of the behavior of several multi-objective metaheuristic methods, using specially chosen test functions, in order to make the search procedure more complicated. The Strength Pareto Evolutionary Algorithm *SPEA* (Zitzler and Thiele, 1998) overcame *MOGA* and was found to be the algorithm that better obtained the Pareto optimal set. In this paper, *SPEA* was chosen as search method to identify the rotor unbalance (magnitude, phase and position) and the load on the bearings, based on how good a set of these parameters is in approximating the simulated orbit in the bearings to the experimental data.

Once the unknown model parameters are estimated, it is possible to approach the mathematical model, and then to obtain more reliable responses for the physical system studied. The use of multi-objective optimization approach returns a Pareto optimal set of solutions, in which no solution is better than other in all objectives simultaneously. Using high level information, it is possible to choose among all of the solutions properly and fit the mathematical model.

2. MATHEMATICAL MODEL OF THE ROTOR-BEARINGS SYSTEM

The dynamic model of the system includes interactions between rotor, shaft and journal bearings and can be divided into two parts: the non-linear hydrodynamic force model due to the journal bearings and the finite element model, which is applied to the shaft and to the lumped mass of the disk.

The model for the non-linear hydrodynamic supporting forces due to the cylindrical journal bearings is based on the work of Capone (1986 and 1991) and is obtained through the direct solution of the Reynolds's Equation [Eq. (01)] for short bearings (Ocvirk (1952)), which neglects the circumferential gradient of pressure distribution. This expression describes the pressure distribution p inside the cylindrical journal bearing for a laminar flux condition and considers the oil thickness h and the axial gradient z, due to the losses of lubricating fluid of the short journal bearing. τ is the nondimensionalized time; ϑ is the cylindrical coordinate, R is the bearing radius, L is the bearing length and μ is the oil film viscosity.

$$\frac{\partial}{\partial\vartheta}\left(h^3\frac{\partial p}{\partial\vartheta}\right)+\left(\frac{R}{L}\right)^2\cdot\frac{\partial}{\partial z}\left(\frac{h^3}{\mu}\frac{\partial p}{\partial z}\right)=\frac{\partial h}{\partial\vartheta}+2\frac{\partial h}{\partial\tau} \tag{1}$$

Figure 1 shows the bearings parameters and the adopted reference system. The geometric parameters of the bearing are: radial clearance C, axial length L and radius R. R_s is the shaft radius, P is the bearing load, α is the work angle, e is the distance between the bearing and the shaft centers and ω is the rotating speed.

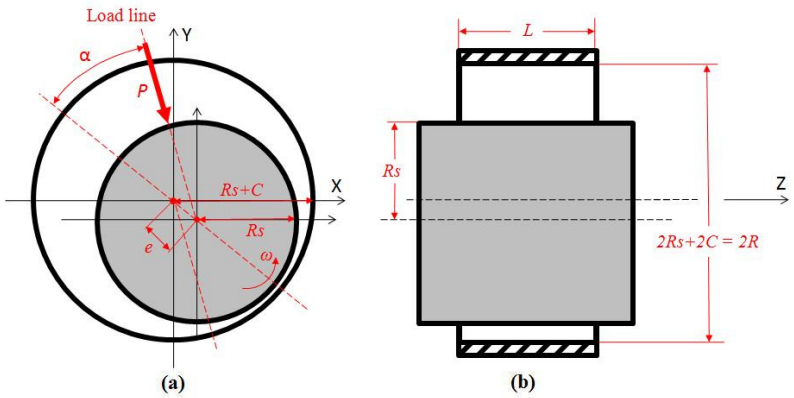

Fig. 1 – Bearing parameters and reference system. (a) Front view; (b) Side view.

The pressure gradient in circumferential direction can be neglected for short journal bearing in relation to the axial gradient (Childs, 1993). Therefore, the result of the differential equation with this simplification is given by Eq. (2), where *D* is the bearing diameter.

$$p(\vartheta,z)=\frac{1}{2}\cdot\left(\frac{L}{D}\right)^2\cdot\left[\frac{(x-2\dot{y})\cdot sin(\vartheta)-(y+2\dot{x})\cdot cos(\vartheta)}{1-x\cdot cos(\vartheta)-y\cdot sin(\vartheta)^3}\right]\cdot(4z^2-1) \tag{2}$$

In order to determine the hydrodynamic forces Fh_x and Fh_y generated by the oil film pressure distribution, the shaft contact area $dA=Rd\vartheta\cdot Ldz$ is considered in Eq. (3), where the functions *V, G* and *F* are defined below. The work angle α is given by Eq. (4). The displacements *x* and *y*, respectively, in the horizontal and vertical directions, are nondimensionalized by the radial clearance of the bearing.

$$\boldsymbol{f_h}=\begin{Bmatrix}f_{hx}\\f_{hy}\end{Bmatrix}=-\mu\omega\cdot\left(\frac{R^2}{C^2}\right)\cdot\left(\frac{L^2}{D^2}\right)\cdot(RL)\cdot\frac{[(x-2\dot{y})^2+(y+2\dot{x})^2]^{\frac{1}{2}}}{(1-x^2-y^2)}\cdot\begin{Bmatrix}3x\cdot V(x,y,\alpha)-sin(\alpha)\cdot G(x,y,\alpha)-2\,cos(\alpha)\cdot F(x,y,\alpha)\\3y\cdot V(x,y,\alpha)-cos(\alpha)\cdot G(x,y,\alpha)-2\,sin(\alpha)\cdot F(x,y,\alpha)\end{Bmatrix} \tag{3}$$

where $V(x,y,\alpha)=\dfrac{2+(y\cdot cos(\alpha)-x\cdot sin(\alpha))\cdot G(x,y,\alpha)}{(1-x^2-y^2)}$; $F(x,y,\alpha)=\dfrac{x\cdot cos(\alpha)+y\cdot sin(\alpha)}{(1-x^2-y^2)}$ and

$$G(x,y,\alpha)=\int_{\alpha}^{\alpha+\pi}\frac{dv}{1-x\cdot cos(v)-y\cdot sin(v)}=\frac{\pi}{\sqrt{1-x^2-y^2}}-\frac{2}{\sqrt{1-x^2-y^2}}\cdot tg^{-1}\left(\frac{y\cdot cos(\alpha)-x\cdot sin(\alpha)}{\sqrt{1-x^2-y^2}}\right)$$

$$\alpha=tg^{-1}\left(\frac{y+2\dot{x}}{x-2\dot{y}}\right)-\frac{\pi}{2}\cdot sign\left(\frac{y+2\dot{x}}{x-2\dot{y}}\right)-\frac{\pi}{2}\cdot sign(y+2\dot{x}) \tag{4}$$

The system excitation force is due to the unbalanced mass *m* and its eccentricity *ε,* as expressed in Eq. (5). The unbalance phase is given by the angle φ and the unbalance node location in the finite element model determines its position in the excitation force vector.

$$\boldsymbol{f_u}=\begin{Bmatrix}\vdots\\f_{u_x}\\f_{u_y}\\\vdots\end{Bmatrix}=m\varepsilon\omega^2\cdot\begin{Bmatrix}\vdots\\cos(\omega t-\varphi)\\sin(\omega t-\varphi)\\\vdots\end{Bmatrix} \tag{5}$$

Figure 2a gives a simplified version of the rotor-bearings system. A finite element method (Fig. 2b) is used to determine the mass **M**, stiffness **K** and gyroscopic **G** matrices, considering the shaft and the concentrated mass of the rotor. The shaft damping matrix **C** contains a first part that is proportional to the stiffness matrix and a second part that contains the gyroscopic effects (**C** = β·**K**+ω·**G**). Bearings 01 and 02 and the lumped mass are located at nodes 3, 9 and 6, respectively, in Fig. 2b. Red arrows indicate the hydrodynamic or unbalance forces. The expected unbalance position is at node 6. L_j is the length of the bearing; L_b is the length of the beam elements, as well as L_1.

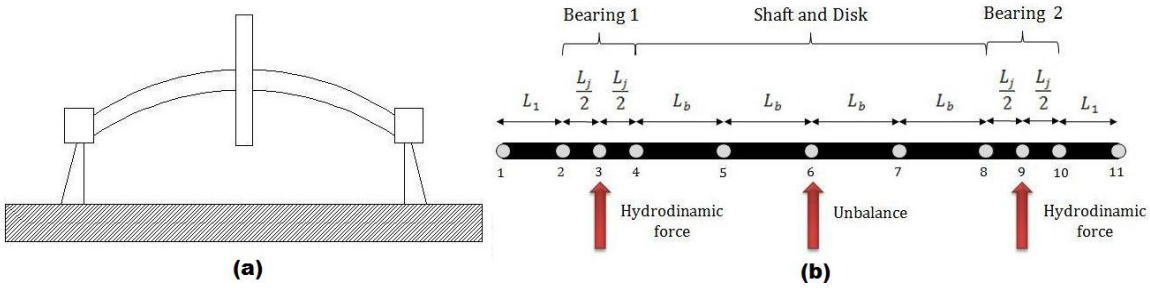

Figure 2. Description of the system. (a) Horizontal rotor physical model; (b) Horizontal rotor finite element model.

The differential equation of motion of the system is given by Eq. (6), which takes into account the hydrodynamic forces $\boldsymbol{f_{h\mu}}$, the unbalanced forces $\boldsymbol{f_u}$ and the rotor weight $\boldsymbol{w}$. The generalized coordinates vector of the flexible rotor is $\boldsymbol{q}^T=\{X_1,\ Y_1,\ \vartheta_{x1}\ ,\ \vartheta_y\ \ldots\ X_{node},\ Y_{node},\ \vartheta_{x\_node}\ ,\ \vartheta_{y\_node}\}$ and considers all the degrees of freedom of the rotating system (displacements and angles of each node), including the journal displacement in each bearing.

$$\boldsymbol{M\ddot{q}+C\dot{q}+Kq=f_{h_\mu}+f_u+w} \tag{6}$$

Equation (6) considers the hydrodynamic forces $\boldsymbol{f_h}$ in Eq. (3) using the oil viscosity μ, which can be found in tables provided by the oil manufacturer for the measured operating temperature of the bearings. In order to identify the load on the bearings, the viscosity was made variable in the search algorithm, i.e., it was obtained a modified viscosity μ_m in each bearing and direction. Thus, it was possible to obtain the hydrodynamic force vector using the modified viscosities and the load on the bearings, as in Eq. (7).

$$\boldsymbol{f_{h_\mu}} = \boldsymbol{f_{h_{\mu m}}} + \boldsymbol{f_{load}} \tag{7}$$

Isolating the viscosity in $\boldsymbol{f_{h\mu}}$ and $\boldsymbol{f_{h\mu m}}$, it is possible to obtain the relation between them [Eq. (8)] and identify the load on the bearings [Eq. (9)] substituting Eq. (8) into Eq. (7).

$$\boldsymbol{f_{h_\mu}} = \mu \cdot \boldsymbol{f} \quad \text{and} \quad \boldsymbol{f_{h_{\mu m}}} = \mu_m \cdot \boldsymbol{f}, \quad \text{so} \quad \boldsymbol{f} = \frac{\boldsymbol{f_{h_\mu}}}{\mu} = \frac{\boldsymbol{f_{h_{\mu m}}}}{\mu_m} \tag{8}$$

$$\boldsymbol{f_{load}} = \boldsymbol{f_{h_\mu}} - \boldsymbol{f_{h_{\mu m}}} = \left(\frac{\mu}{\mu_m} - 1\right) \cdot \boldsymbol{f_{h_{\mu m}}} \tag{9}$$

The solution of the equation of motion [Eq. (6)] in the time domain is obtained through the application of a numerical method. For this case, Newmark's method, according to Bathe and Wilson (1976), was chosen, as it is a well known algorithm for solving nonlinear problems in structural dynamics.

3. OBJECTIVE FUNCTION

The tuning method contains objective functions that involves all the control variables obtained experimentally: orbit of the shaft in the bearings, as well as the phase of the orbit. These control variables depend on the variables that are fitted in the optimization process (rotor unbalance (magnitude, phase and position)) and the modified viscosity for each bearing and direction. A diagnosis technique, based on Childs (1993), is proposed to characterize the elliptical shape of the orbit. This analysis includes the degree of ellipticity, given by the Shape and Directivity Index (*SDI*), the dimension of the major axis of the orbit a and its inclination with respect to the horizontal axis θ, as shown in Fig. 3. The orbit phase ν is the angle of the first point of the orbit in one period (point S). This parameter is hardly influenced by the unbalance phase φ.

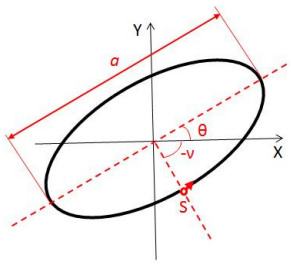

Figure 3. Orbit-related parameters.

The displacement in x and y directions are shown in Eq. (10), in which *xs*, *xc*, *ys*, *yc* are the first order Fourier coefficients, that are also used to obtain the angle θ in Eq. (11).

$$x = x_c \cdot cos(\omega t) + x_s \cdot sin(\omega t) \quad ; \quad y = y_c \cdot cos(\omega t) + y_s \cdot sin(\omega t) \tag{10}$$

$$\theta = \frac{1}{2} \cdot tg^{-1}\left(\frac{2 \cdot (x_c \cdot y_c + x_s \cdot y_s)}{{x_c}^2 + {x_s}^2 - {y_c}^2 - {y_s}^2}\right) \tag{11}$$

The degree of ellipticity *SDI* is given by Eq. (12), as well as the dimension of the largest and the smallest dimension of the ellipse, a and b respectively.

$$SDI = {}^{b}/_{a} \ , \quad \text{with} \quad a = \sqrt{C_1 + \sqrt{{C_2}^2 + {C_3}^2}} \ ; \quad b = \frac{1}{a} \cdot (x_c \cdot y_s - x_s \cdot y_c)$$
$$\text{where} \quad C_1 = \frac{1}{2} \cdot (x_c^2 + y_c^2 + x_s^2 + y_s^2) \ ; \ C_2 = \frac{1}{2} \cdot (x_c^2 + y_c^2 - x_s^2 - y_s^2) \ ; \ C_3 = x_c \cdot x_s + y_c \cdot y_s \tag{12}$$

The difference between the experimental and the adjusted orbits can be approximated by the difference between their parameters *SDI, a,* θ and v. The minimization process of each one of these differences is considered as an objective function to be minimized, constituting a multi-objective problem. This way, Eq. (13) presents the objective functions of the proposed problem. The orbits are adjusted for two nodes, represented by the two bearings.

$$f_\theta = \sum_{1}^{node} \left| \frac{\theta_{exp} - \theta_{adj}}{2\pi} \right|; \quad f_a = \sum_{1}^{node} \left| \frac{a_{exp} - a_{adj}}{2C} \right|; \quad f_{SDI} = \sum_{1}^{node} \left| SDI_{exp} - SDI_{adj} \right|; \quad f_v = \sum_{1}^{node} \left| \frac{v_{exp} - v_{adj}}{2\pi} \right| \tag{13}$$

4. EXPERIMENTAL SETUP

The experimental setup consists of two hydrodynamic bearings and a lumped mass assembled in the central position of the shaft (Fig. 4), similar to a Laval rotor. It is composed of a 12-mm-diameter steel shaft with an effective length of 600mm between the bearings. The concentrated mass consists of a chromed steel disk with an external diameter of 95mm, thickness of 43mm and mass of 2.34kg. A pair of cylindrical hydrodynamic bearings is used to support the shaft, made in bronze, with a length of 20mm, radial clearance of 90μm and L/D ratio of 0.64. The bearings are lubricated with AWS 32 oil. A flexible coupling joins the rotor shaft and the driving-motor, next to bearing 01. The nominal frequency of the electric motor lies in the range of 1 to 60 Hz and the rotor support structure can be considered rigid in this operational range of frequencies.

Figure 4. Experimental bench and data acquisition instrumentation.

The experimental bench measurements are obtained by means of sensors installed at the bearings. The displacements of the shaft inside the bearing are recorded by proximity sensors. The vibrations of the bearing supports are monitored by means of accelerometers. The oil temperature is measured with thermocouples. An optical sensor is installed between the flexible coupling and the driving-motor and it is used as a trigger to start the signal acquisition and also used as a reference for the experimental phase calculation.

5. MULTI-OBJECTIVE METAHEURISTIC METHOD

5.1. Genetic Algorithm

Genetic algorithms, first proposed by Holland (1975), are a random search technique that simulates the process of genetic evolution. Each parameter is codified by a gene using an appropriate representation. The corresponding genes for all of the parameters form a chromosome that is capable of describing a solution of the problem. Each individual is evaluated in each generation based on its fitness, i.e., on how good it is in solving the problem. A group of chromosomes representing several individual solutions of the problem includes a population in which an individual with the best characteristics (closer to the global solution) has more chance of being selected to reproduce. The evolution is executed using a series of stochastic operators to manipulate the genetic code, in other words, with the evolution of the search, the population includes better solutions and, eventually, converges.

The selection operator is an important phase of GA because it selects the most capable individuals to reproduce and participate in the next generation (iteration). The individual's probability to be selected depends on its fitness. The objective of this process is to make copies of good solutions and eliminate bad solutions in a population, while maintaining the size of the population constant.

Crossover is an operator that applies crossings to combine different individuals' genes to produce the offspring, as shown in Fig. 5a. It usually selects two chromosomes - called parents - and random portions of the genetic material to

exchange among them in order to generate new chromosomes - called new individuals (children). The parents are selected among the existent chromosomes in the population, preferably in order of its fitness, so that the new individuals can inherit the parents' good characteristics. Applying iteratively the crossing operator, genes of chromosomes with better fitness will more frequently appear in the population.

The mutation operator is applied to randomly modify the new individuals' code, as shown in Fig. 5b. The mutation is a critical element of a GA because, instead of guiding the population for the convergence, as the crossover operator, it reintroduces the genetic diversity in the population and allows the search process to escape from local optima.

After using the genetic operators, the new individuals are inserted in a new population and the procedure is restarted.

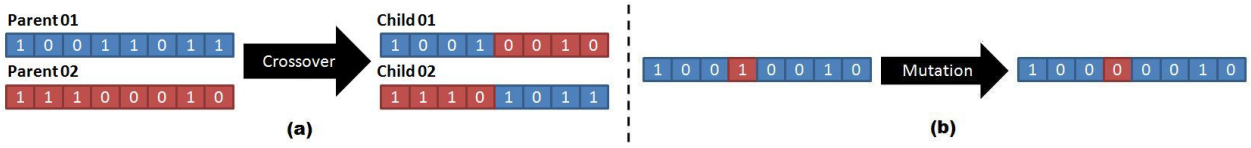

Figure 5. Genetic Operators. (a) One point crossover; (b) One point mutation.

5.2. Multi-objective problems

Real engineering problems usually involve simultaneous consideration of multiple performance criteria, in which objectives are non-commensurate and are frequently in conflict among them. Optimize the problem with regard to only one objective eventually can generate an inadmissible solution in relation to other objectives. Once there is more than one conflicting objective, a single best solution usually does not exist and the concept of Pareto dominance can be applied. An individual *A* is said to dominate an individual *B* if solution *A* is no worse than *B* in any objective and if *A* is strictly better than *B* in at least one objective (Deb, 2001). In other words, '*B* is dominated by *A'* or '*A* dominates *B'*. The definition of the Pareto optimal set of solutions refers to the set of solutions that are not dominated by any other solution in the given problem domain. If a multi-objective problem has multiple optimal solutions, the multi-objective genetic algorithms have a great probability of identifying and storing them in its final population.

5.3. Strength Pareto Evolutionary Algorithm (*SPEA*)

The Strength Pareto Evolutionary Algorithm (*SPEA*) is a multi-objective genetic algorithm proposed by Zitzler and Thiele (1998). This evolutionary algorithm has been intensely tested and applied to several engineering problems inside industrial and scientific areas. It explicitly maintains an external population that stores the best solutions found until the present generation (iteration), a characteristic known as elitism. *SPEA*'s external population is updated in each generation: the old non-dominated solutions are compared with the recently found solutions and the non-dominated resultant set is chosen to form the new external population. To avoid that the external population becomes overcrowded, due to the continuity for several generations of the process of non-dominated solutions identification, the authors limited the external population to a chosen size N_e. Deb (2001) affirms that the choice of N_e must be careful for the successful working of the algorithm, however, the researchers of *SPEA* concluded that a reason of 1:4 between N_e and the current population size N is satisfactory for most of the problems. When the amount of non-dominated individuals is inferior to N_e, all solutions are maintained, when it is superior, not all elites can be allocated in the external population and a clustering algorithm is proposed. That algorithm preserves the elites of less populated areas of the search space, improving the diversity of solutions. The Euclidean distance between all solutions of the expanded external population is calculated and the closer solutions are eliminated from the external population until the external population reaches only N_e solutions.

In this algorithm, a smaller fitness represents a better solution. In order to evaluate the fitness of each found solution, a strength parameter *Si* is assigned to each one of the members of the external population. This value is proportional to the number of individuals n_i of the current population that a member of the external population dominates. The division by *(N+1)* in Eq. (14) guarantees that the maximum strength parameter in an iteration of the algorithm is less than the unit. Then, the fitness of each solution in the current population can be calculated: it will be always the sum of the strength parameters of all external population members that dominates the analyzed solution plus one. So, the fitness [Eq. (15)] of any current population member is greater than any fitness (strength) of an external population member, or rather, any *Fj* will always be greater than the maximum *Si*.

$$S_i = \frac{n_i}{N+1} \tag{14}$$

$$F_j = 1 + \sum_{i \in P_e \,\wedge\, i \prec j} S_i \tag{15}$$

Subsequently, the selection operator can be applied to the entire population (current and external). For *SPEA*, a binary tournament selection was proposed, where two randomly chosen solutions are compared. The one with a better fitness will be chosen, what emphasizes the elite solutions. The procedure is repeated until all the population has been compared (N tournaments). The genetic operators of crossover and mutation are then applied to find a new current population. The external solutions participate in the genetic operators of selection and crossover in order to guide the future populations through good areas of the search space. This way, its evolutionary advantage can be explored, what increases considerably the chances of generating a set of solutions closer to the real Pareto front. After these procedures, a new population of size N is created.

6. SEARCH ALGORITHM

Step 1. Randomly generate an initial population. The binary representation (genotype) is used for each individual of the population and carries information about the unbalance (magnitude, phase and position) and about the unknown loads acting on both bearings.

Step 2. Transform genotype into phenotype: convert the binary string of each individual in real values.

Step 3. Solve the differential equation of motion of the system [Eq. (6)] to obtain the simulated orbits and forces, considering each individual of the population as a solution. Calculate the objective functions to solve Eq. (13), i.e., compare the simulated results to the experimental data.

Step 4. Use the Pareto dominance to discover the non-dominated solutions in the current population and add them to the external population.

Step 5. Use the Pareto dominance to locate the non-dominated solutions in the modified external population and eliminate the dominated ones.

Step 6. If the size of the external population after step 5 is larger than the chosen limit N_e, use the clustering algorithm to reduce its size to that limit.

Step 7. Assign the strength parameter to each solution of the external population, so that the fitness of each solution of the current population can be calculated.

Step 8. Apply the selection operator: use the binary tournament selection to accomplish N tournaments among the combined current and external populations.

Step 9. Apply the crossover operator: randomly choose a crossing point and two individuals to be crossed, considering the combined population. However, individuals from the external population cannot be altered.

Step 10. Apply the mutation operator: randomly choose an individual of the current population and the bits that will be the mutation points.

Step 11. If the total number of generations (stop criterion) was not reached, go to next generation and return to Step 2: through the use of the genetic operators, a new population, which is probably closer to the final solution, is created. This new population must be evaluated and, if possible, improved.

7. RESULTS AND DISCUSSION

Experimental results were obtained for 4 constant rotation speeds (22, 22.5, 23.5 and 24.5 Hz). The resonance of the physical system was identified to be located at 23Hz and it was not possible to obtain experimental data for this speed. For all measured speeds, the measured operating temperature of the oil was 25ºC, which returns an oil viscosity of $\mu = 0.052$ Pa·s.

After the experimental analysis, the search algorithm was applied to the problem. A set of GA parameters returned good results for this problem was: total number of generations: 50; population size N: 32; external population size N_e: 8; crossover probability: 0.7; mutation probability: 0.35; mutation rate: 0.25. The search algorithm was applied for each rotation speed individually. For each case, it returned a Pareto set of solutions (that contained the unbalance parameters and the modified viscosity in each bearing), in which it was not possible to select the best one. As the unbalance of the machine is the same for all speeds, individuals with the same set of unbalance parameters were selected (Tab. 01). It was expected to obtain the unbalance position at node 6, as it is the location of the rigid disk (Fig. 2).

Table 1. Unbalance parameters estimated by the heuristic method.

Magnitude $m \cdot \varepsilon$ [Pa·s]	Position (node)	Phase φ [Degrees]
$1.14 \cdot 10^{-4}$	6	-75

The comparison between the orbits from the selected solutions and the experimental results for all considered speeds are shown in Fig. 6. The simulated orbits returned a good approximation for the experimental results from bearing 2. The differences between the orbits in bearing 1, especially for the *SDI* parameter, can be explained because bearing 1 is close to a flexible coupling, which joins the rotor shaft and the driving-motor. The presence of the coupling adds more stiffness in that area and, consequently, more difficulties in the modeling procedure.

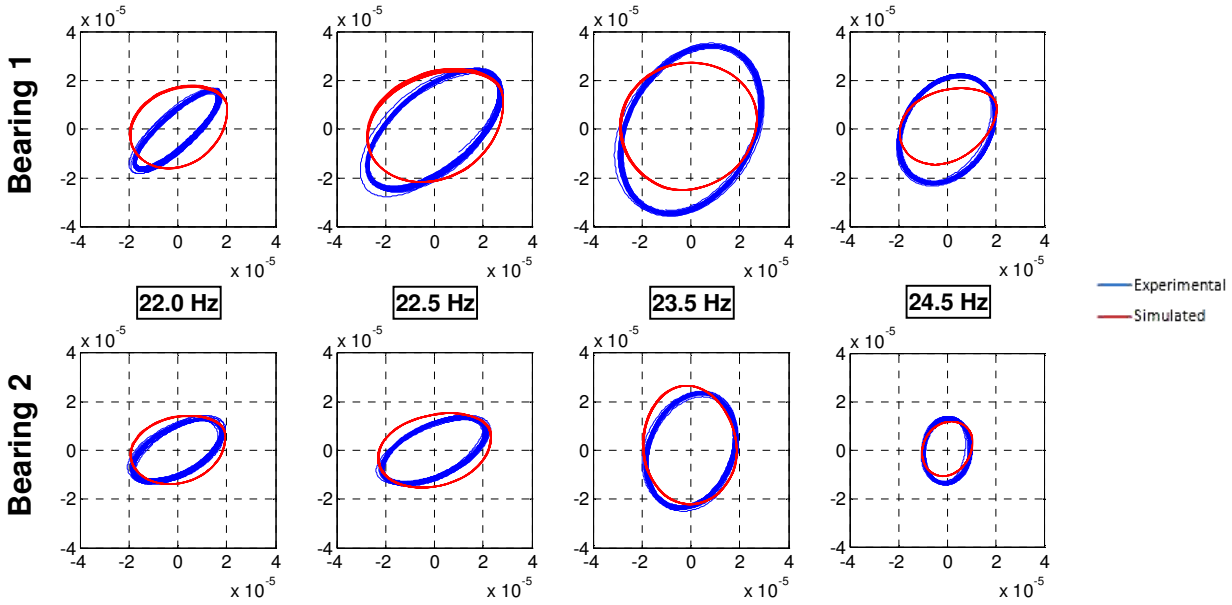

Figure 6. Experimental and simulated bearing orbits for each rotating speed.

It can be noticed that the method presents difficulties in finding the angle θ, for orbits with a more circular shape, i.e., orbits with a *SDI* value closer to the unit. Figure 7 compares the experimental orbit phase ν_{exp} (blue) and the simulated orbit phase ν_{adj} (red). Good approximations were obtained, especially for bearing 1 at 22Hz. However, for bearings 1 and 2 at 24.5Hz the difference was considerable: 41.4º and 101.6º, respectively.

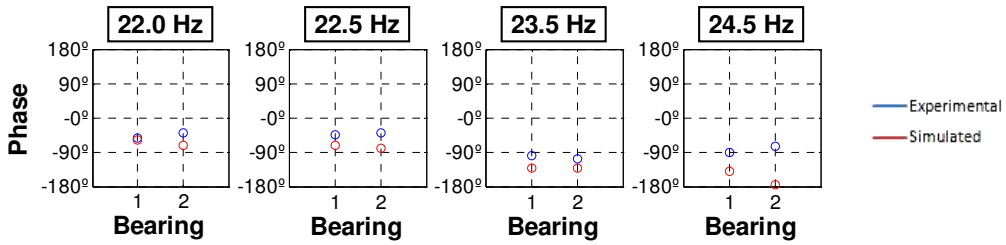

Figure 7. Experimental ν_{exp} and simulated ν_{adj} orbit phase for each rotating speed.

Table 2 presents the objective functions from Eq. (13) and the correspondent contribution from each bearing. It can be noticed from Tab. 2 and confirmed by Fig. 6 that the solution for bearing 2 at 22.5 Hz was the one that best approximated the larger axis of the ellipses. Bearing 1 at 24.5 Hz and bearing 2 at 23.5Hz presented the best adjustment for the SDI, however bearing 1 at 24.5 Hz a not so good approximation for θ. Bearing 2 at 22.5 Hz returned the smaller difference among experimental and simulated angle θ, closely followed by bearing 1 at 22.5 Hz and both bearings at the speed 22.0 Hz. As confirmed by Fig. 7, bearing 1 at 22.0 Hz showed the best adjustment for the phase angle ν.

The same experimental setup used in this work was used by Castro *et al.* (2008) for 22.5 Hz and the unbalance magnitude identified by the *MOGA* algorithm ($1.24 \cdot 10^{-4}$ Pa·s) was close to the value showed in Tab. 1. It can also be

mentioned that the two individuals analyzed in that work for 22.5 Hz are non-dominated if compared to the ones identified in this work for that speed. However, in that work only f_a , f_{SDI} and f_θ were considered in the search algorithm.

Table 2. Objective functions for each rotational speed and bearing.

	22.0 Hz			22.5 Hz		
	Bearing 1	Bearing 2	Total	Bearing 1	Bearing 2	Total
f_a	$2.03 \cdot 10^{-2}$	$9.80 \cdot 10^{-3}$	$\mathbf{0.30 \cdot 10^{-1}}$	$2.91 \cdot 10^{-2}$	$1.43 \cdot 10^{-3}$	$\mathbf{0.31 \cdot 10^{-1}}$
f_{SDI}	$4.70 \cdot 10^{-1}$	$2.00 \cdot 10^{-1}$	$\mathbf{6.71 \cdot 10^{-1}}$	$1.98 \cdot 10^{-1}$	$1.40 \cdot 10^{-1}$	$\mathbf{3.84 \cdot 10^{-1}}$
f_θ	$5.40 \cdot 10^{-2}$	$5.22 \cdot 10^{-2}$	$\mathbf{1.06 \cdot 10^{-1}}$	$5.54 \cdot 10^{-2}$	$4.32 \cdot 10^{-2}$	$\mathbf{0.99 \cdot 10^{-1}}$
f_v	$1.63 \cdot 10^{-2}$	$8.82 \cdot 10^{-2}$	$\mathbf{1.05 \cdot 10^{-1}}$	$7.63 \cdot 10^{-2}$	$1.16 \cdot 10^{-1}$	$\mathbf{1.92 \cdot 10^{-1}}$
	23.5 Hz			24.5 Hz		
	Bearing 1	Bearing 2	Total	Bearing 1	Bearing 2	Total
f_a	$4.47 \cdot 10^{-2}$	$9.55 \cdot 10^{-3}$	$\mathbf{0.54 \cdot 10^{-1}}$	$1.59 \cdot 10^{-2}$	$5.87 \cdot 10^{-3}$	**0.22·10-1**
f_{SDI}	$2.47 \cdot 10^{-1}$	$3.69 \cdot 10^{-2}$	$\mathbf{2.84 \cdot 10^{-1}}$	$2.23 \cdot 10^{-2}$	$1.82 \cdot 10^{-1}$	$\mathbf{0.20 \cdot 10^{-1}}$
f_θ	$1.22 \cdot 10^{-1}$	$7.30 \cdot 10^{-2}$	$\mathbf{1.95 \cdot 10^{-1}}$	$1.55 \cdot 10^{-1}$	$4.59 \cdot 10^{-1}$	$\mathbf{6.14 \cdot 10^{-1}}$
f_v	$6.50 \cdot 10^{-2}$	$1.07 \cdot 10^{-1}$	$\mathbf{1.72 \cdot 10^{-1}}$	$1.15 \cdot 10^{-1}$	$2.82 \cdot 10^{-1}$	$\mathbf{3.97 \cdot 10^{-1}}$

Figure 8 shows the hydrodynamic forces (F_h) and the load (F_a) in RMS value for each bearing and direction (x and y). Closer to the resonance the hydrodynamic forces in both directions presented higher values. If bearing 1 and 2 are compared, it can be noticed that the hydrodynamic forces have a greater value in bearing 1. The bearing loads on bearings 1 and 2 presented a different behavior after resonance due to the presence of the flexible coupling next to bearing 1.

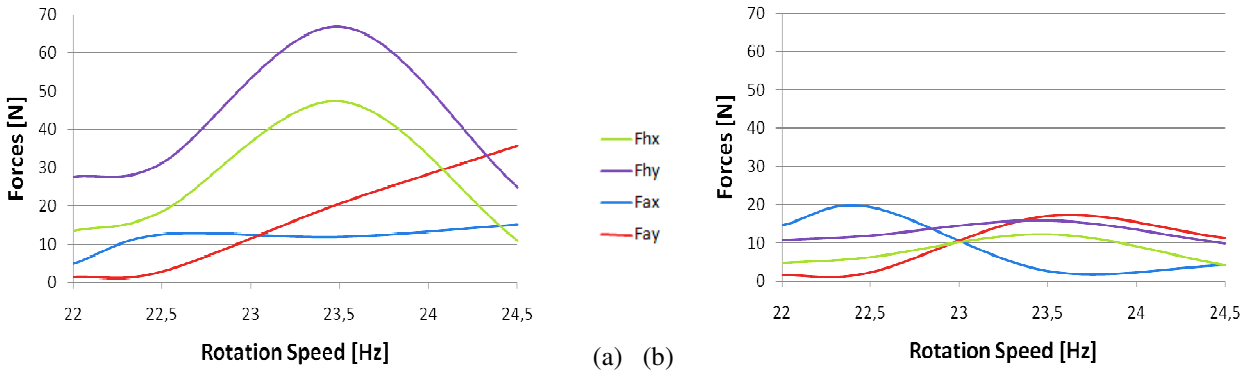

Figure 8. RMS value for the hydrodynamic and load forces on the bearings. (a) Bearing 1; (b) Bearing 2.

8. CONCLUSIONS

In this paper, a multi-objective genetic algorithm, based on Zitzler and Thiele's *SPEA* (1998) was applied to adjust a non-linear rotating system model in time domain by identifying its unbalance parameters (magnitude, position and phase) and load on the bearings. Experimental and simulated results were compared by their bearings orbit-related parameters (objective functions). Four rotation speeds – two before and two after resonance – were considered since it is a critical stage of the machine operation and still the algorithm was able to satisfactorily adjust the experimental data. The differences between adjusted and experimental data can be explained by some variables that are not considered in the model, like motor-shaft coupling.

The adjustment method is useful for the analysis of rotating machines due to eventual limitations of the mathematical models in representing the real structure in a complete way. A very promising approach was obtained for the unbalance identification using only the displacement measurements in the bearings, which makes the method particularly interesting to practical applications in real machines.

9. ACKNOWLEDGEMENTS

The authors thank FAPESP, CNPq and CAPES (Brazil) for the support for this research.

10. REFERENCES

Bachschmid, N., Pennacchi, P. Vania, A., 2004, "Diagnostic Significance of Orbit Shape Analysis and its Application to Improve Machine Faults Detection". Journal of the Brazilian Society of Mechanical Sciences and Engineering n. 24, pp. 200-208.

Bathe, K. J., Wilson, E. J., 1976, "Numerical Methods in Finite Element Analysis", Prentice-Hall, Inc. Englewood Cliffs, New Jersey.

Capone, G., 1986, "Orbital motions of rigid symmetric rotor supported on journal bearings". La Meccanica Italiana, n. 99, pp. 37-46.

Castro, H.F., Idehara, S.J., Cavalca, K.L, Dias, M. Jr., 2004, "Updating Method Based on Genetic Algorithm applied to nonlinear journal bearing Model". Proceedings of ImechE 2004 – 8th International Conference on Vibrations in Rotating machinery, Swansea, UK, pp. 1-10.

Castro, H.F., Cavalca, K. L., Mori, B. D., 2005, "Journal Bearing Orbits Fitting Method with Hybrid Meta-heuristic Method". Proceedings of the COBEM 2005, Ouro Petro, Brazil, pp. 1 – 10.

Castro, H.F., Pennacchi, P., Cavalca, K.L, 2007, "Parameter estimation of a rotor-bearing system using genetic algorithm and simulated annealing", Proceedings of XII International Symposium on Dynamic Problems of Mechanics, Ilha bela, Brazil, pp.1-10.

Castro, H. F., Cavalca, K.L., Camargo, L.W.F., 2008, "Multi-Objective Genetic Algorithm Application in Unbalance Identification for Rotating Machinery". Proceedings of ImechE 2008 – 9th International Conference on Vibration in Rotating Machinery. London, v. 2, pp. 885-897.

Cavalca, K.L., Idehara, S.J., Dedini, F.G., Pederiva, R. 2001, "Experimental nonlinear Model updating Applied in Cylindrical Journal Bearings". Proceedings of ASME 2001 design Engineering Technical Conference, Pittsburg, USA, pp. 1-9

Childs, D., 1993, "Turbomachinery Rotor dynamics. Phenomena, Modeling and Analysis", John Wiley & Sons, New York, p.476.

Capone, G., 1991, "Descrizione analitica del campo di forze fluidodinamico nei cuscinetti cilindrici lubrificati", L.Energia Elettrica, n. 3, pp. 105-110.

Deb, K., 2001, "Multi-Objective Optimization using Evolutionary Algorithms". John Wiley and Sons, Chichester, 515p.

Fonseca, C.M. and Fleming, P.J., 1993, "Multiobjective genetic algorithms", IEE colloquium on 'Genetic Algorithms for Control Systems Engineering' (Digest No. 1993/130), London, UK.

Goldberg D., 1989, "Genetic Algorithms in Search and Machine Learning". Reading. Addinson Wesley.

Holland, J.H., 1975, "Adaptation in Natural and Artificial Systems". University of Michigan Press, Ann Arbor.

Kirkpatrick, S., C.D. Gelatt Jr., M.P. Vecchi, 1982, "Optimization by Simulated Annealing", IBM Research Report RC 9355.

Lund, J. W. 1987, "Review of the concept for dynamic coefficients for fluid film journal bearings". ASME Journal of Tribology Vol. 109, pp.38–41.

Ocvirk, F. W., 1952, "Short-Bearing Approximation for Full Journal Bearings", National Advisory Committee for Aeronautics (NACA), Technical Report TN 2808.

Reynolds, O., 1886, "On the Theory of Lubrication and its Application to Mr. Beauchamp Tower's Experiments, including an Experimental Determination of the Viscosity of Olive Oil". Philosophical Transactions of Royal Society of London, Series A, Vol. 177, Part 1, 1886, pp.157-234.

Tower, B., 1883, "First report on friction experiments". Proc. Inst. Mech. Eng, pp. 632–659.

Tower, B., 1885, "Second report on friction experiments", Proc. Inst. Mech. Engineers, pp. 58-70.

Zitzler, E., Thiele, L. 1998, "An evolutionary algorithm for multiobjective optimization: The strength Pareto approach". Technical report 43, Zürich, Switzerland: Computer Engineering and Networks Laboratory (TIK), Swiss Federal Institute of Technology (ETH).

Zitzler, E., Deb, K., Thiele, L., 2000, "Comparison of Multiobjective Evolutionary Algorithms: Empirical Results". In Evolutionary Computation Journal 8 (2), pp 125-148.

11. RESPONSIBILITY NOTICE

The authors are the only responsible for the printed material included in this paper.